Pollen-tube tip growth requires a balance of lateral propagation and global inhibition of Rho-family GTPase activity

Jae-Ung Hwang[1,*], Guang Wu[1,*], An Yan[1], Yong-Jik Lee[1], Claire S. Grierson[2] and Zhenbiao Yang[1,‡]

[1]Department of Botany and Plant Sciences and Center for Plant Cell Biology, Institute for Integrative Genome Biology, University of California-Riverside, Riverside, CA 92521, USA
[2]School of Biological Sciences, University of Bristol, BS8 1UG, UK
*These authors contribute equally to this work.
‡Author for correspondence (zhenbiao.yang@ucr.edu)

Accepted 9 November 2009
Journal of Cell Science 123, 340-350 Published by The Company of Biologists 2010
doi:10.1242/jcs.039180

Summary

Rapid tip growth allows for efficient development of highly elongated cells (e.g. neuronal axons, fungal hyphae and pollen tubes) and requires an elaborate spatiotemporal regulation of the growing region. Here, we use the pollen tube as a model to investigate the mechanism regulating the growing region. ROPs (Rho-related GTPases from plants) are essential for pollen tip growth and display oscillatory activity changes in the apical plasma membrane (PM). By manipulating the ROP activity level, we showed that the PM distribution of ROP activity as an apical cap determines the tip growth region and that efficient tip growth requires an optimum level of the apical ROP1 activity. Excessive ROP activation induced the enlargement of the tip growth region, causing growth depolarization and reduced tube elongation. Time-lapse analysis suggests that the apical ROP1 cap is generated by lateral propagation of a localized ROP activity. Subcellular localization and gain- and loss-of-function analyses suggest that RhoGDI- and RhoGAP-mediated global inhibition limits the lateral propagation of apical ROP1 activity. We propose that the balance between the lateral propagation and the global inhibition maintains an optimal apical ROP1 cap and generates the apical ROP1 activity oscillation required for efficient pollen-tube elongation.

Key words: Pollen tube, Tip growth, Rho GTPase

Introduction

The formation of elongated tubular cells is a critical developmental process required for a number of eukaryotic cells to perform their characteristic functions: (1) neurons differentiate, producing long axons essential for unilateral signal propagation over a long distance; (2) fungal hyphae grow to an extensive length to explore nutrients in the environment; (3) the root trichoblasts develop a long tubular root hair with enormous surface area for efficient uptake of water and nutrients in the soil; and (4) pollen grains on the stigma develop pollen tubes that penetrate into female tissues and deliver sperm to eggs. The formation of these highly elongated tubular structures is dependent on extreme polar growth or 'tip growth' (Bushart and Roux, 2006; Govek et al., 2005; Hepler et al., 2001). The growth signal needs to be confined to a small apical area and to be continuously regenerated to support the continuous tip growth. However, the underlying molecular basis is poorly understood.

A hypothesis for cell polarity control has emerged from recent studies in budding yeast and migrating cells: spatial cues break the symmetry to induce local activation of Rho GTPases and Rho-dependent polarization of the actin cytoskeleton, and the asymmetry of Rho and actin cytoskeleton is stabilized by positive-feedback loops (Butty et al., 2002; Ozbudak et al., 2005; Wedlich-Soldner et al., 2003; Weiner et al., 2002; Xu et al., 2003). Although this general principle for polarity control appears to be conserved in evolution, it is unclear whether it underlies the control of the extension of hyphae, axons or pollen tubes over a long distance. In these systems, a tight spatial control and rapid regeneration of growth signal is required to maintain a relatively constant region of growth for the formation of highly elongated cylindrical cells.

For sexual reproduction, pollen tubes extend rapidly (up to 1 cm/hour) from the surface of pistils to the ovule, guided by signals from the female tissues (Franklin-Tong, 1999; Lord and Russell, 2002). Previous studies have established a crucial role for the Rho-family GTPase ROP1 in the control of polar growth in pollen tubes (Fu et al., 2001; Gu et al., 2005; Gu et al., 2003; Hwang et al., 2005; Kost et al., 1999; Li et al., 1999; Lin and Yang, 1997). Blocking ROP1 signaling by expressing dominant-negative ROP1 or by microinjecting anti-ROP1 antibody inhibited pollen-tube tip growth, suggesting that ROP1 is essential for pollen-tube tip growth (Kost et al., 1999; Li et al., 1999; Lin and Yang, 1997). ROP1 preferentially localizes to the apical region of the pollen-tube plasma membrane (PM), and active ROP1 is distributed as an apical cap in the PM apex (Gu et al., 2003; Hwang et al., 2005). This apical cap of ROP1 activity shows spatiotemporal dynamics with maximum activity preceding a growth peak during the oscillatory growth of pollen tubes (Hwang et al., 2005). In turning pollen tubes, the apical cap relocalizes to the future site of growth. These results support a role for the apical cap of ROP1 activity in the spatiotemporal control of pollen-tube growth. However, the underlying mechanisms for the formation of the apical ROP1 cap and for its dynamics are unknown. In this work, we aimed to investigate why the spatiotemporal dynamics of the apical ROP1 activity is required for rapid and continuous tip growth and how it is achieved.

Journal of Cell Science

Results

Biphasic effect of an increase in apical ROP1 activity on pollen-tube growth

Apically localized ROP1 activity is essential for tip growth in pollen tubes (Li et al., 1999; Lin and Yang, 1997). However, over-activation of ROP1 by overexpressing wild-type (WT) ROP1 or a constitutively-active ROP1 mutant (CA-rop1) induces growth depolarization, resulting in short and swollen pollen tubes (Kost et al., 1999; Li et al., 1999). To further investigate the relationship between the level of apical ROP1 activity and pollen-tube growth and polarity, we manipulated an increase of apical ROP1 activity to various levels by transiently expressing *Arabidopsis* ROP1 in tobacco pollen tubes (Fig. 1). Transiently overexpressed *Arabidopsis* ROP1 increases the amount of active ROP1 in the tobacco pollen-tube apex (Gu et al., 2005; Hwang et al., 2005). We quantified active ROP1 amount and distribution using an active ROP1 reporter, GFP-RIC4ΔC (RIC4 truncated in the C-terminus) (Hwang et al., 2005). RIC4 is a CRIB-motif-containing ROP1 effector, which promotes the assembly of F-actin (Gu et al., 2005; Wu et al., 2001). The C-terminus truncation (RIC4ΔC) does not affect the specific binding ability of RIC4 to GTP-ROP1 but loses the effector function (Gu et al., 2005; Hwang et al., 2005). Fluorescence resonance energy transfer (FRET) analysis shows that the distribution of RIC4ΔC to the apical PM faithfully reflects the ROP1 activation as an apical cap in the pollen-tube apical PM (Hwang et al., 2005).

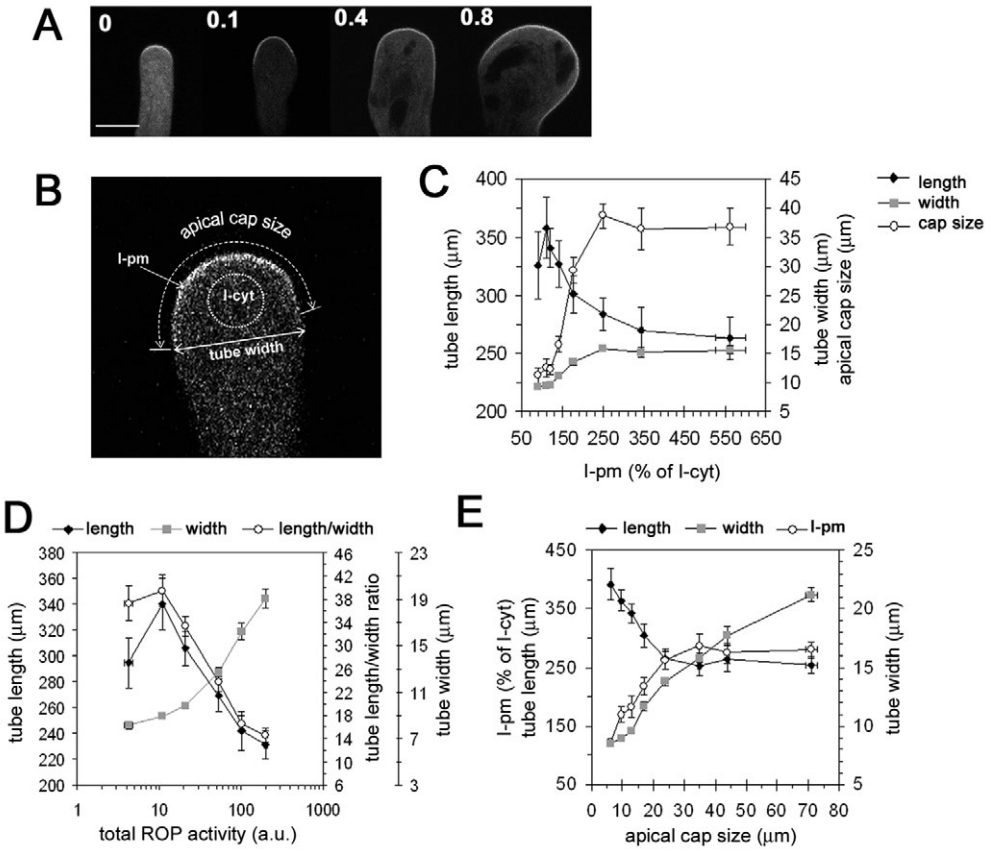

Fig. 1. A biphasic relationship between the increase in apical ROP1 activity and pollen-tube growth. To determine how varying levels of the apical ROP1 activity affect pollen-tube growth behavior, different amounts (0-0.8 μg) of the *LAT52::ROP1* construct were transiently expressed in tobacco pollen tubes. The apical ROP1 activity was monitored as described in the text from the medial longitudinal confocal images of pollen tubes. The size of the active ROP1 cap and the mean and total ROP1 activity at the tube apical PM were measured. A total of 558 pollen tubes from five independent transformation experiments were analyzed and grouped according to the three features of the apical ROP1 activity, and their relationships with pollen-tube elongation (tube length) and polarity (tube width) were assessed. (**A**) Representative images of the longitudinal medial section for tubes co-expressing GFP-RIC4ΔC and ROP1. Varying amounts of input ROP1 constructs (0-0.8 μg) are indicated at the top of each tube. Scale bar: 10 μm. (**B**) A schematic demonstrating how ROP1 activity in the apical cap was quantified. When a pollen tube has a width greater than that of control tubes, it is considered to display growth depolarization. The size of active ROP1 cap was quantified by measuring the distance of the PM region with distinct GFP-RIC4ΔC intensity, as indicated. The mean ROP1 activity was estimated as the mean GFP intensity within the apical cap standardized with the mean cytosol GFP intensity (I-pm in % of I-cyt). The total ROP1 activity in the apical cap was estimated by multiplying I-pm/I-cyt by the cap size. (**C**) The relationship between pollen-tube growth behavior (tube elongation and growth polarity changes) and the mean ROP1 activity in the apical cap (I-pm). The tubes were grouped according to I-pm (*x*-axis), of which mean values were plotted against those of pollen-tube length, width, and the size of active ROP1 cap (*y* axes) (mean values ± s.e.m., $n \geq 50$ each data point.). (**D**) The relationship between pollen-tube growth behavior and the total ROP1 activity in the apical cap. The tubes were grouped according to the total ROP1 activity (*x*-axis, arbitrary unit, a.u.), which was plotted against pollen-tube length, width, and the length/width ratio (*y* axes) (mean ± s.e.m., $n \geq 50$ each data point.). (**E**) The size of the active ROP1 cap is linearly correlated with the tube width. Pollen tubes were grouped and analyzed according to the cap size, which was plotted against I-pm, tube length and width (mean ± s.e.m., $n \geq 50$ each data point). The Pearson correlation coefficient between 558 pairs of cap size and tube width was 0.80 (significance at $P<0.0001$), indicating that the active ROP1 cap determines the growing region.

On the assumption that a pollen tube is a cylinder with a hemisphere at the tip and that active ROPs (GFP-RIC4ΔCs) are localized to the hemisphere PM, forming a symmetric gradient from the very summit, the pollen-tube growth rate (net surface area increase per unit time) is linearly proportional to the elongation rate of pollen tubes. Likewise, the broadness and the amount of active ROP localized to the hemisphere are linearly proportional to those of GFP-RIC4ΔC localization observed in a single median section of the pollen-tube apical PM. Therefore, in this study we examined three features of the apical ROP1 activity (broadness, mean level and total level) from median sectioned CLSM images of GFP-RIC4ΔC localization to the pollen-tube apical PM in comparison with the linear pollen-tube elongation (pollen-tube length) and growth polarity (pollen-tube width) (Fig. 1). GFP-RIC4ΔC forms an apical cap in the median section of pollen-tube apical PM (Fig. 1A). The broadness of the active ROP1 distribution in the apical PM was measured as the distance of the apical PM region with distinct GFP-RIC4ΔC localization ('cap size' of GFP-RIC4ΔC apical cap, Fig. 1B). The mean ROP1 activity in the apical PM was measured as the mean GFP-RIC4ΔC intensity in the apical cap ('I-pm', Fig. 1B). I-pm was standardized as a percentage of the mean GFP-RIC4ΔC intensity in the cytosol ('I-cyt', Fig. 1B) to minimize variation due to GFP-RIC4ΔC expression difference. The total amount of active ROP1 in the pollen-tube apical PM was estimated by multiplying I-pm/I-cyt by 'cap size' ('total ROP1 activity', Fig. 1B).

From 558 pollen tubes expressing GFP-RIC4ΔC and various amounts of ROP1, we quantified ROP1 activity and analyzed pollen-tube elongation (tube length) and growth polarity (tube width) according to the three aspects of ROP1 activity (Fig. 1C-E). We found an interesting biphasic relationship between ROP1 activity increase and pollen-tube growth (Fig. 1C-D). A slight increase in the mean and total apical ROP1 activity was associated with a promotion in pollen-tube elongation without a significant change on the tube width (Fig. 1C,D). However, further increases in ROP1 activity were associated with a reduction in tube elongation coupled with an expansion in tube width, i.e. growth depolarization. We also found that the tube width increase is linearly proportional to that of the cap size (Fig. 1E, Pearson correlation coefficient=0.80). The correlation of the tube width with the active ROP1 cap size strongly supports the hypothesis that the apical cap of active ROP1 determines the growth region. Taken together, our results show that efficient tube elongation requires an optimum level of apical ROP1 activity. Increasing active ROP1 up to this optimum level promotes pollen-tube elongation. When ROP1 is present at levels above the optimum, however, the apical ROP1 cap is enlarged, resulting in growth depolarization and reduction in elongation. In our observations, promotion of pollen-tube elongation was induced by only a slight increase in ROP1 activity. Thus, in vivo levels of ROP1 activity in WT pollen tubes optimal for pollen-tube elongation might be near saturation.

The active ROP1 cap is rapidly regenerated in the apical PM during oscillatory tip growth

In vitro cultured pollen tubes display oscillatory tip growth in the absence of any external cues, producing a highly elongated pollen tube. This implies that a self-organizing mechanism for the generation of growth region (the apical ROP1 cap) exists to support rapid continuous tip growth. To gain insights into how the active ROP1 cap is generated and maintained, we analyzed spatial and

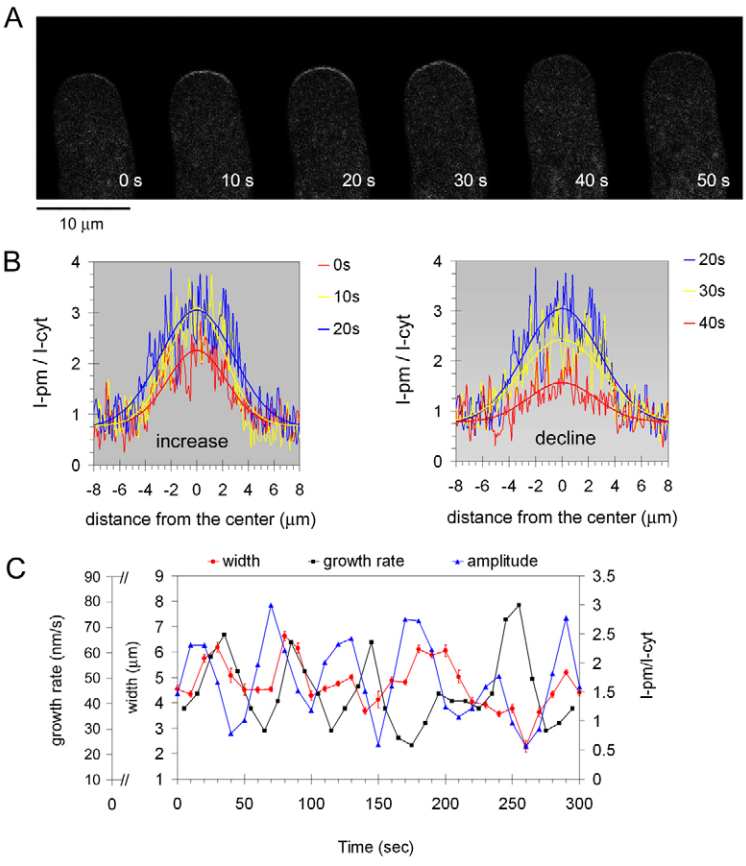

Fig. 2. The apical cap of active ROP1 is generated through localized ROP1 activation followed by its lateral spreading in the pollen-tube apex, whereas global inhibition is involved in the removal of the apical cap. To track spatiotemporal dynamics of the apical ROP1 activity, GFP-RIC4ΔC localization to the tip was time-lapse imaged at 10 second intervals from a pollen tube that grew the oscillatory tip growth. (**A**) A representative cycle of the apical ROP1 activity oscillation (0-50 seconds). GFP-RIC4ΔC starts to arise from the center of the tube apical PM and propagates rapidly to form the apical cap maximum (0-20 seconds). After reaching the peak, GFP-RIC4ΔC localization in the apical PM decreases (20-40 seconds). The next active ROP1 cap initiates in the center of a previous apical cap (50 s). Numbers indicate time elapsed (seconds) from time 0. (**B**) Intensity profiles of GFP-RIC4ΔC in the apical cap. GFP-RIC4ΔC intensity (I-pm) was line-scanned from CLSM images in A. Standardized I-pm values with I-cyt are displayed in thin lines according to the distance from the center, and the corresponding Gaussian fit curves are presented in thick lines (Origin 7, $y=y0 + (A/(w*\sqrt{(\pi/2)}))*\exp(-2*((x-xc)/w)^2)$; *y*, I-pm/I-cyt; *x*, position in the apical PM; y0, offset; xc, center; yc, y at center; amplitude, yc-y0; w, width at (yc-y0)/2; A, area). The graph on the left shows the intensity profiles during ROP1 activity increase (0-20 seconds), and the graph on the right shows intensity profiles during ROP1 activity decline (20-50 seconds). (**C**) Oscillation curves of amplitude and width from B, with tip growth rate from the same pollen tube as in A. The peaks of amplitude (maximum ROP1 activity) are ahead of those of width (at half amplitude). A similar temporal lag of an increase in width was observed in four individual pollen tubes with ~60 second period oscillations.

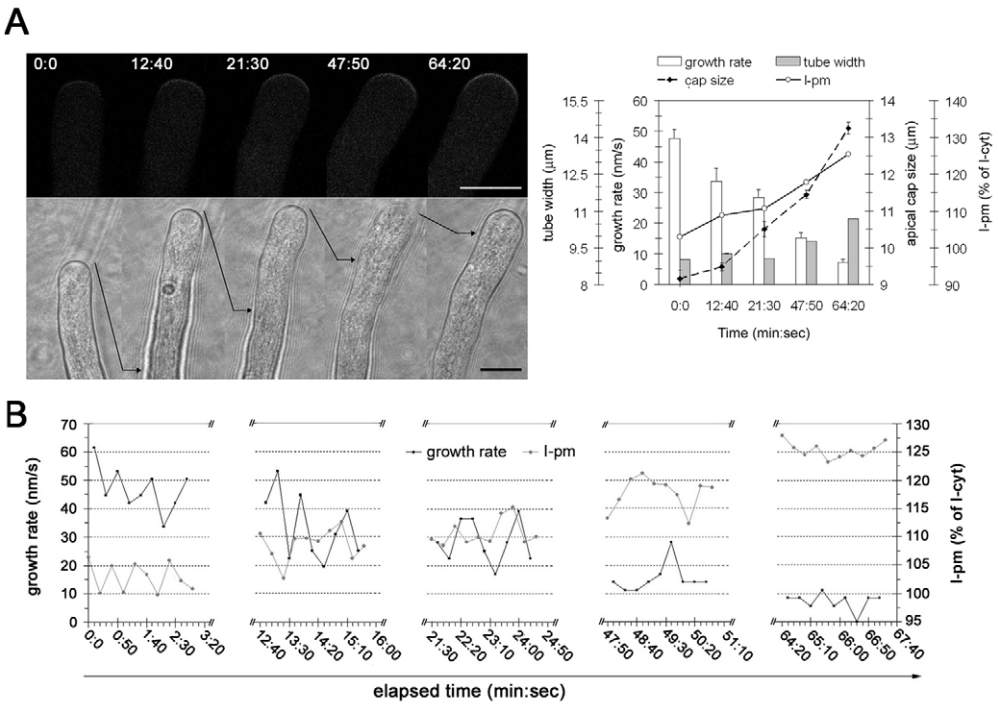

Fig. 3. The gradual enlargement of the size of the active ROP1 cap is accompanied by a dampening of the apical ROP1 activity oscillation, because ROP1 activation dominates ROP1 inhibition. A small amount of ROP1 constructs (50-100 ng) was used to overexpress ROP1 to a moderate level. Over 2.5 hours of bombardment, normally growing transgenic pollen tubes were chosen for time-lapse imaging. (**A**) Left, representative images showing the apical ROP1 activity (top) and pollen tubes (bottom). Numbers are the elapsed times (minutes:seconds) from the beginning of recording (0:0). At each time point, time-lapse imaging (20 second intervals) was performed for 3 minutes. The net tube elongation between time points is indicated with arrowed lines. Scale bars: 10 μm. Quantitative data of pollen-tube growth and the apical ROP1 activity (mean ± s.e.m.) measured for 3 minutes is shown on the right. The growth rate, I-pm, and the cap size are significantly increased from 12:40, whereas the tube width is apparently wider from time 47:50 (Student's *t*-test, $P<0.05$). (**B**) The oscillations of the apical ROP1 activity (I-pm) and tip growth rate were dampened as the apical ROP1 activity increased. At the beginning (0:0 in A, left), the pollen tube exhibited the normal oscillatory tip growth and apical ROP1 activity (growth rate and I-pm). As the ROP1 activity was apparently amplified by ROP1 overexpression, the apical ROP1 activity (both I-pm and the cap size) progressively increases (A). The increase in the apical ROP1 activity is accompanied by a gradual dampening of tip growth oscillations (B) and tip expansion (A).

temporal changes in the apical ROP1 activity in tobacco pollen tubes that exhibit rapid oscillatory tip growth. The active ROP1 cap was found to be continuously generated in the apex of rapidly growing pollen tubes slightly ahead of each cycle of tip growth oscillation (Hwang et al., 2005; Fig. 2). Similar oscillation patterns of apical ROP1 cap generation were observed in all 12 individual growing tubes analyzed.

Careful analysis revealed several characteristics of the dynamic changes in the oscillatory apical ROP1 cap. First, the ROP1 activity tended to increase from a small region of the tube apical PM as shown in Fig. 2A. An increase in ROP1 activity usually began near the center of the PM apex without an apparent change in the cap size (0-10 seconds, Fig. 2A,B). Second, this increase in ROP1 activity rapidly spreads laterally to the whole apex of the PM (10-20 seconds, Fig. 2A,B). This lateral propagation of apical ROP1 activity was not due to the overall GFP intensity increase in the PM. Profiles of GFP-RIC4ΔC intensity in the apical PM follow a bell-shaped Gaussian distribution (Fig. 2B). To more clearly illustrate the temporal relationship between the initial rise of ROP1 activity in the center and the subsequent lateral spreading, the amplitude and width (at half amplitude) of GFP-RIC4ΔC distribution curves were calculated by using Gaussian curve fit function. We observed that the amplitude of GFP-RIC4ΔC localization to the apical PM increases temporally ahead of the GFP-RIC4ΔC width increase in all rapidly growing pollen tubes examined (Fig. 2C, $n=12$). For tubes displaying tip growth oscillation with a ~60 second period, the peaks of width were 8.8±1.2 seconds (equivalent to 60±8.8 degrees out of phase) behind those of amplitude ($n=4$). This lateral propagation could be due to the stabilization of PM-localized GFP-RIC4ΔC or de novo activation of inactive ROP1. We found that the FRAP behavior of PM-localized GFP-RIC4ΔC was nearly identical to the oscillatory changes in GFP-RIC4ΔC (supplementary material Fig. S1), suggesting that the lateral propagation of PM-localized GFP-RIC4ΔC is most likely due to de novo activation of ROP1 in the apical PM.

Third, the rise of ROP1 activity to the maximum was followed by its downregulation, so that the apical ROP1 activity did not spread to the PM region flanking the apex. We reasoned that either or both of two possible modes of negative regulation, which are not mutually exclusive, could limit ROP1 activity to the apex: lateral and global inhibition. In lateral inhibition, ROP1 negative regulators act at the flanks of the tip and limit the lateral propagation of active ROP1. If this mode of ROP1 downregulation were predominant, we would expect a preferential reduction of ROP1 activity in the region flanking the center of the PM apex. By contrast, we found that the decline of ROP1 activity tended to be even throughout the apex (20-40 seconds, Fig. 2A,B). This clearly supports a global inhibition

mechanism(s), by which ROP1 negative regulators equally deactivate ROP1 in all regions of the PM wherever ROP1 is active.

Based on the above observations, we propose that the apical active ROP1 cap is generated by the lateral propagation of locally initiated ROP1 activation and maintained by a global inhibition mechanism(s). According to this hypothesis, we predicted that a balanced interplay between lateral propagation of ROP1 activation and its global inhibition would be necessary for the oscillation of the ROP1 apical cap and thus for efficient tube elongation. As a first step in testing this prediction, we transiently expressed a small amount of ROP1 construct (50-100 ng) in tobacco pollen tubes to increase ROP1 activation. As shown in Fig. 3, when time-lapse imaging began 2.5 hours after bombardment, the pollen tube displayed rapid oscillatory growth (time 0:0). At this time, GFP-ROP1 started to accumulate to a detectable level (data not shown), but insufficient to affect the oscillatory tip growth. However, the apical ROP1 activity (both I-pm and cap size) increased gradually afterwards (time 12:40 to 64:20) as more ROP1 protein accumulated (Fig. 3A). The increase in apical ROP1 activity (both I-pm and cap size) was temporally associated with a significant reduction in tube elongation rate (time 12:40-64:20) and followed by the increase in tube width (time 47:30 to 64:20) (Fig. 3A, right panel). In addition, as ROP1 activity increased, the oscillation of apical ROP1 activity and tip growth was dampened and eventually was completely lost when the size of the apical ROP1 cap was dramatically enlarged (Fig. 3B). These results suggest that ROP1 overactivation over the optimum level overrides the negative regulation, causing the lateral spreading of apical ROP1 activity unchecked, which subsequently leads to the loss of ROP1 activity oscillation and growth depolarization.

Global inhibition by GDI and GAP counteracts the propagation of the apical ROP1 activity

We sought to assess whether negative regulators of ROP, RopGAPs and RhoGDIs, participate in the global ROP1 inhibition in the tube apex. When this work was initiated, three RhoGDIs and six GAPs (RopGAPs) had been reported in *Arabidopsis* (Bischoff et al., 2000; Wu et al., 2000). Our pollen RT-PCR analysis detected transcripts of all three RhoGDIs and transcripts of RopGAP1 and RopGAP3 (Fig. 4A). We primarily used RhoGDI1 and RopGAP1 in the transient expression experiment in tobacco pollen tubes, because they were shown to regulate ROP1 and closely related ROPs in vitro or in vivo (Bischoff et al., 2000; Carol et al., 2005; Fu et al., 2001; Hwang et al., 2005; Wu et al., 2000). Moreover, they appeared functionally redundant with their respective relatives based on their overexpression phenotype and localization in tobacco pollen tubes (supplementary material Fig. S2).

We first examined the cellular localization of GFP-fused RhoGDI1 and RopGAP1. If these negative regulators act laterally, we would expect them to be localized in the PM region flanking the apical cap of active ROP1. If they act as global inhibitors, we would expect them to localize to the cytoplasm uniformly or to the apical PM. GFP-RhoGDI1 was exclusively localized to the cytosol. GFP-RopGAP1 was found both in the cytoplasm and the apical PM (Fig. 4B). The other two RhoGDIs (RhoGDI2a and RhoGDI2b) and RopGAP3 displayed similar localization to RhoGDI1 and RopGAP1, respectively (supplementary material Fig. S2). These localization patterns are consistent with our hypothesis that RopGAPs and RhoGDIs act as global inhibitors.

We next investigated whether their overexpression globally reduced the apical ROP1 activity in pollen tubes. As expected,

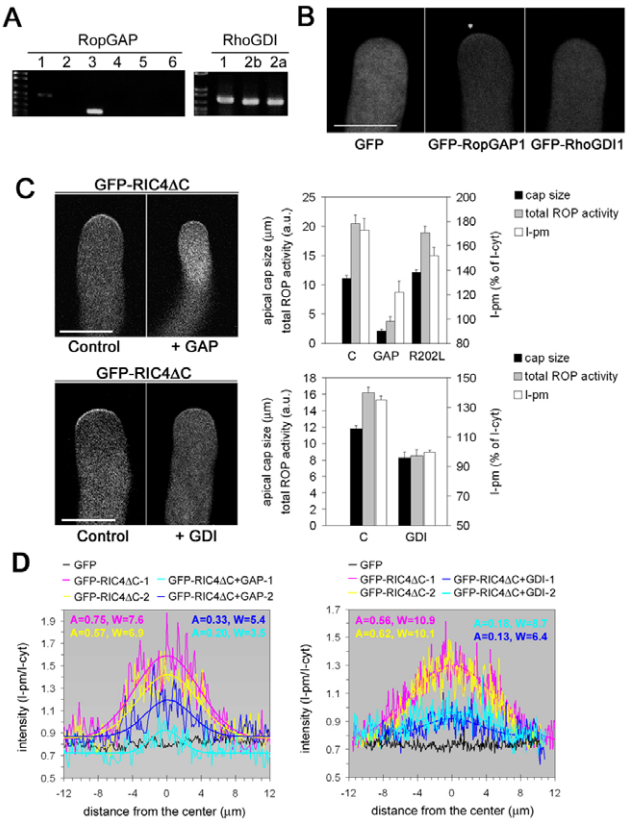

Fig. 4. RopGAP1 and RhoGDI1 globally inhibit the apical ROP1 activity in tobacco pollen tubes. Various constructs were transiently expressed in tobacco pollen, and transformed tubes were analyzed. C, control; GAP, RopGAP1; R202L, RopGAP1(R202L); GDI, RhoGDI1. (**A**) RT-PCR analysis detected the transcripts of RopGAP1, RopGAP3, RhoGDI1, RhoGDI2a and RhoGDI2b in *Arabidopsis* pollen. No transcripts for RopGAP4, 5, and 6 were detected in the assay. Pollen RNA was isolated, and RT-PCR was performed. 40 and 35 cycles of amplifications (94°C for 30 seconds, 58°C for 30 seconds, and 72°C for 1 minute) were performed for RopGAPs (GAP) and RhoGDIs (GDI), respectively. (**B**) Representative localization patterns of GFP-RopGAP1 and GFP-RhoGDI1. GFP-RopGAP1 is localized both in the cytosol and the tube apical PM (asterisk). GFP-RhoGDI1 localizes only in the cytosol. Scale bar: 10 μm. (**C**) Both RopGAP1 and RhoGDI1 globally inhibit the apical ROP1 activity. Overexpression of either RopGAP1 (top panels) or RhoGDI1 (bottom panels) significantly reduced the total ROP1 activity in the tube apex, which results in the reduction in both the average ROP1 activity (I-pm) and the size of apical ROP1 cap (cap size). Left panels show representative images of GFP-RIC4ΔC localization. Right panels show quantitative data from three independent experiments (mean ± s.e.m., n>60 each, P<0.01). In both RopGAP1 and RhoGDI1 cases, reduction in the amount and the cap size of the apical ROP1 activity (see left panels) was associated with a global decrease in GFP-RIC4ΔC intensity in the tube apical PM. In about 50% of RopGAP1-overxpressing tubes, distinct GFP-RIC4ΔC localization to the PM was lost. In these tubes, the cap size was considered to be zero, accounting for the unusually small mean size of the apical ROP1 cap. RopGAP1(R202L) reduced the I-pm slightly, which might result from its CRIB motif competing with RIC4ΔC for active ROP1 interaction. However, the effects of RopGAP1 on the cap size and I-pm were significantly different from those of RopGAP1(R202L) (P<0.05). Scale bars: 10 μm. (**D**) Representative GFP-RIC4ΔC intensity profiles in the apical cap from RopGAP1 (GAP in left panel) or RhoGDI1 (GDI in right panel) expressing pollen tubes in comparison with control tubes (GFP-RIC4ΔC alone or free GFP). As in Fig. 2, GFP-RIC4ΔC intensity (I-pm) was line-scanned from CLSM images and ratios of I-pm/I-cyt are displayed according to the distance from the center, and corresponding Gaussian fit curves are presented. A, amplitude; W, width.

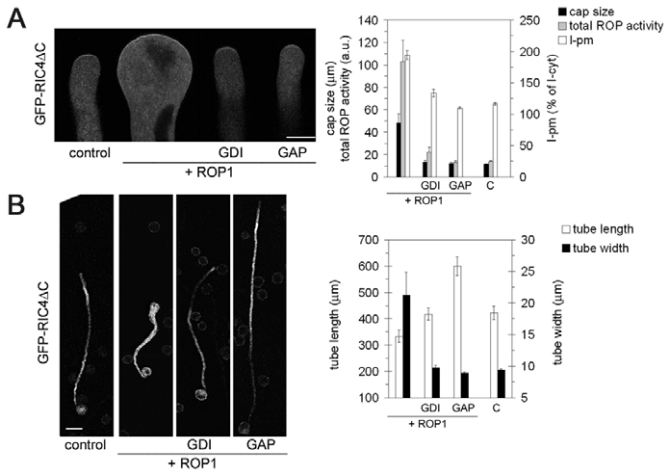

Fig. 5. GAP and GDI suppress the lateral propagation of the apical ROP1 activity. Various constructs were transiently expressed in tobacco pollen, and transformed tubes were analyzed. Control (C), GFP-RIC4ΔC alone or GFP alone; GAP, RopGAP1; GDI, RhoGDI1. (**A**) RopGAP1 and RhoGDI1 co-expression suppressed the enlargement of the apical ROP1 cap induced by ROP1 overexpression. Left, representative images showing tip-localized GFP-RIC4ΔC. Scale bar: 10 µm. Right, quantitative data (mean ± s.e.m., n>30, each). RhoGDI and RopGAP significantly inhibited the increases in I-pm, cap size, and total ROP activity induced by ROP1 overexpression (P<1.0×10^{-4}). Similar results were obtained in three independent experiments. (**B**) Coexpression of RopGAP1 or RhoGDI1 suppressed the growth depolarization induced by ROP1 overexpression (P<0.005). Left, representative pollen-tube images. Scale bar: 50 µm. Right, quantitative data (mean ± s.e.m., n>30, each). Similar results were obtained in three independent experiments.

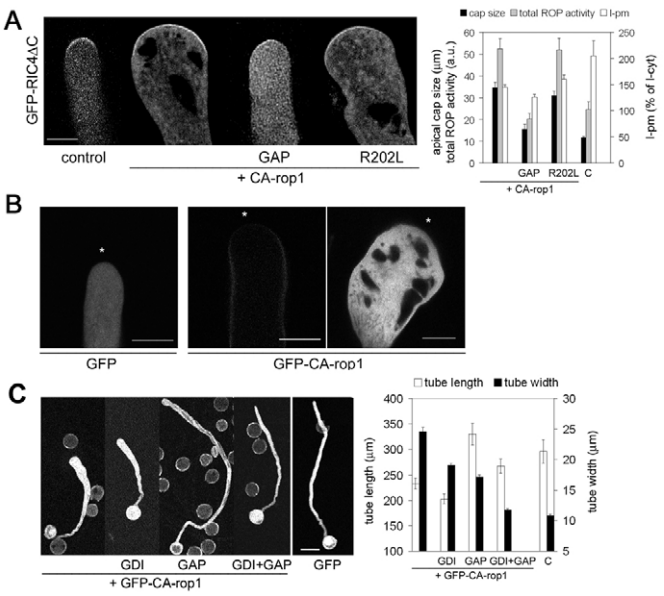

Fig. 6. CA-rop1 induces the enlargement of the active ROP1 cap and growth depolarization by promoting the activation of endogenous ROP1. Different constructs were transiently expressed in tobacco pollen. Control (C), expressing GFP-RIC4ΔC alone; GAP, RopGAP1; R202L, RopGAP1(R202L). (**A**) CA-rop1-induced enlargement of the active ROP1 cap is suppressed by RopGAP1. The apical ROP1 activity was visualized with GFP-RIC4ΔC in tubes expressing CA-rop1 alone or co-expressing CA-rop1 and RopGAP1 or RopGAP1(R202L). CA-rop1 dramatically increased the total apical ROP1 activity and the size of the active ROP1 cap, and this increase was suppressed by RopGAP1 coexpression (P<0.005), but not by RopGAP1(R202L) coexpression. Left, representative images showing GFP-RIC4ΔC localization. Scale bar: 10 µm. Right, quantitative data (mean ± s.e.m., n≥30, each). Similar results were obtained in three independent experiments. CA-rop1 tended to induce a lower I-pm than that in control tubes, probably because of the accumulation of CA-rop1 in the cytosol, which could reduce the pool of GFP-RIC4ΔC available for the PM-localized active ROP1. (**B**) Representative images showing the localization of GFP-CA-rop1 in pollen tubes. In the majority of pollen tubes, GFP-CA-rop1 was found in the cytosol and a small amount was associated with the PM (right). The PM association is clearly seen only in pollen tubes with a low level of GFP-CA-rop1 expression (center). Unlike that of WT-ROP1 (Li et al., 1999; supplementary material Fig. S3), the PM association of GFP-CA-rop1 did not preferentially occur at the PM apex, but rather evenly in the whole PM (22% of cells observed) or preferentially in the PM regions flanking the apex (45%). The images were taken focused on the pollen-tube apex (asterisk). Scale bar: 10 µm. (**C**) Co-expression of RopGAP1 effectively suppressed growth depolarization induced by GFP-CA-rop1. Left, representative pollen-tube images. Scale bar, 50 µm. Right, quantitative data (mean ± s.e.m., n>30, each). RopGAP1 coexpression with GFP-CA-rop1 substantially promoted tube elongation (P<5×10^{-4}) and suppressed growth depolarization (P<5×10^{-12}). Similar results were observed in three independent experiments.

both the I-pm and the cap size of GFP-RIC4ΔC were significantly reduced when either RopGAP1 or RhoGDI1 was transiently overexpressed (Fig. 4C). In both cases, the total ROP1 activity reduction was associated with a global decline of active ROP1 through the apical PM (see representative images in Fig. 4C and intensity profiles in Fig. 4D). Accordingly, overexpression of RopGAP1 or RhoGDI1 decreased both pollen-tube length and width (supplementary material Fig. S2). These observations support the participation of RhoGDI and RopGAP in the global ROP1 inhibition rather than lateral inhibition, because lateral inhibitors are expected to predominantly reduce the cap size and the tube width.

We then tested whether the global inhibition by RopGAP and RhoGDI could balance the propagation of the apical ROP1 activation by co-expressing ROP1 with either of the negative regulators. We hypothesized that an increase in ROP1 global inhibition would counteract an increase in ROP1 activation, producing the apical ROP1 activity similar to that in WT pollen tubes. Overexpression of ROP1 dramatically enlarged the apical ROP1 cap, inducing growth depolarization (Fig. 5). The total ROP1 activity (measured by either I-pm or the cap size) was dramatically increased when pollen was transformed with 0.5 µg of ROP1 construct (Fig. 5A). Coexpression of RhoGDI1 or RopGAP1 almost completely restored the apical ROP1 activity and polarized tip growth to those in control tubes (Fig. 5A,B). In both cases of RhoGDI1 and RopGAP1 coexpression, the cap size and I-pm of tip-localized GFP-RIC4ΔC were reduced to similar levels as control tubes, further supporting the function of RhoGDI1 and RopGAP1 as global inhibitors of the apical ROP1 activation (Fig. 5A). The apparent coordinated effect of RopGAP1 and RhoGDI1 could be explained by the fact that they regulate the deactivation and PM association of ROP1, respectively, but detailed mechanism for this coordination remains to be explored.

Transient expression of a constitutively active ROP1 [ROP1 (G15V), CA-rop1] also induced a dramatically enlarged active ROP1 cap and growth depolarization (Fig. 6A). Similarly to the effect of stable expression in *Arabidopsis* (Li et al., 1999), growth depolarization induced by transiently expressed CA-rop1 was much

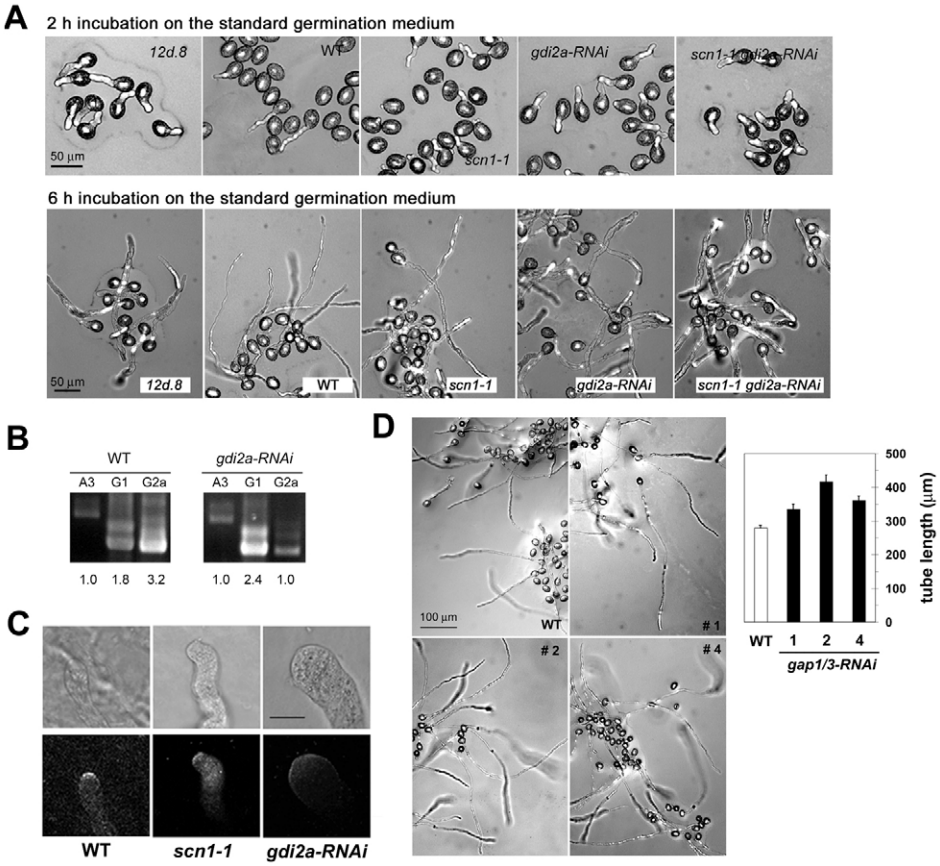

Fig. 7. Role of RhoGDIs and RopGAPs in the control of ROP1 activation in the pollen-tube apex in *Arabidopsis*. (**A**) Loss of RhoGDI2a function (*gdi2a-RNAi*) caused growth depolarization as did *GFP-ROP1* overexpression, whereas LOF of RhoGDI1 (*scn1-1*) resulted in slightly wavy pollen-tube growth. Representative pollen-tube images of *GFP-ROP1ox* (*12d.8*), WT, *scn1-1*, *gdi2a-RNAi* and *scn1-1 gdi2a-RNAi* (top, 2 hours and bottom, 6 hours). (**B**) Pollen RT-PCR analysis of RhoGDI2a transcript level (G2a) in *gdi2a-RNAi* pollen in comparison with that of WT pollen. Actin3 (A3) and RhoGDI1 (G1) are used as an internal control. Numbers at the bottom indicate relative band intensities compared with that of Actin3. (**C**) Localization of endogenous ROP was depolarized in *gdi2a-RNAi* pollen tubes. Representative images showing endogenous ROP localization to *Arabidopsis* pollen-tube apex, which was visualized with anti-ROP antibody. Scale bar: 10 μm. (**D**) Knockdown of RopGAP1 and RopGAP3 might promote pollen-tube growth, but does not affect growth polarity. Left, representative images of WT or three independent *gap1/3-RNAi* pollen tubes cultured on the germination medium containing 0.5 mM Ca^{2+} for 8-9 hours. Right, quantitative result of *gap1/3-RNAi* pollen-tube growth compared with that of WT (mean ± s.e.m.). The pollen-tube length of *gap1/3-RNAi* lines was longer than that of WT tubes ($n \geq 100$ each, $P < 0.001$).

more severe compared with WT ROP1. The data in Fig. 6 are from pollen tubes 3-5 hours after bombardment with 0.2 μg CA-rop1 construct, compared with 4-7 hours after bombardment with 0.5 μg ROP1 construct shown in Fig. 5. Surprisingly, GFP-tagged CA-rop1 in tobacco pollen tubes exhibited a localization pattern that was very distinct from that of GFP-RIC4ΔC, although GFP-RIC4ΔC was shown to specifically bind and report the localization of active ROP1 (Hwang et al., 2005). In contrast to the enlarged apical cap of GFP-RIC4ΔC in CA-rop1-expressing tubes, GFP-CA-rop1 was primarily accumulated in the cytosol and was weakly associated with the PM in a broad area (Fig. 6B). Furthermore, GFP-CA-rop1 was only weakly associated with or nearly absent in the apical PM in the majority of cells (Fig. 6B and supplementary material Fig. S3). A simple explanation for these differences in localization patterns between RIC4ΔC and CA-rop1 is that CA-rop1 expression induced an increased activation of endogenous ROP1. Consequently the enhanced RIC4ΔC localization to the apical cap was primarily due to its interaction with tip-localized endogenous active ROP1, whose tip localization was dramatically enhanced by CA-rop1 expression.

If the CA-rop1-induced enlargement of the apical ROP1 cap was indeed primarily due to CA-rop1 induction of endogenous ROP1 activation, we would expect that the CA-rop1 phenotype could be suppressed by co-expression with RopGAP1. CA-rop1 is GTPase-dead and insensitive to RhoGAPs (Klahre and Kost, 2006; Li et al., 1999), and thus suppression of the CA-rop1 phenotype by RopGAP1 would support the notion that CA-rop1 is able to induce the activation of endogenous ROP1. As shown in Fig. 6A and 6C, RopGAP1 coexpression indeed suppressed CA-rop1-induced enlargement of the apical ROP1 cap and growth depolarization (Fig. 6A,C). This suppression was not due to simple sequestration of CA-rop1 or blockage of CA-rop1 interaction with its effectors by overexpressed RopGAP1, because a non-catalytic mutant, RopGAP1(R202L), did not suppress CA-rop1-induced changes (Fig. 6A). The interaction of RopGAP to active ROP is primarily dependent on the CRIB motif and the R202L mutation of the conserved catalytic Arg residue does not affect RopGAP1 interaction with ROP1 (Klahre and Kost, 2006) (supplementary material Fig. S2D,E).

Loss of RhoGDI2a function causes the depolarized growth in *Arabidopsis* pollen tubes

To further investigate the role of RhoGDIs in the control of the apical ROP1 activity, we examined *Arabidopsis* mutants, in which *RhoGDI* genes were knocked down or knocked out. Loss of RhoGDI1 function induces depolarization of root hair cells, producing several swollen hairs from a hair-forming cell (Carol et al., 2005; Parker et al., 2000). We examined in vitro cultured pollen tubes from RhoGDI1 mutants (*scn1-1*, *scn1-2* and *scn1-3*) (Carol et al., 2005; Parker et al., 2000). In the first 2-6 hours of culture, *scn1-1* pollen tubes displayed slightly zigzagged tip growth. However, overall pollen-tube growth of *scn1-1* was not significantly different from WT pollen tubes (Fig. 7A). The other *scn1-1* alleles (*scn1-2* and *scn1-3*) showed identical in vitro pollen-tube phenotypes to *scn1-1* (data not shown). The apical localization of endogenous ROPs, which was visualized using anti-ROP1 antibody, did not show obvious depolarization in the *scn1-1* pollen tubes (Fig. 7C). It is unclear how *scn1* mutants generated the slightly wavy

pollen-tube growth. Loss of RhoGDI1 might cause temporal disturbance in the active ROP1 cap, which can induce temporal growth arrest and growth resumption in random. RhoGDI2b is reported to be highly expressed in mature pollen (Genevestigator, https://www.genevestigator.ethz.ch/). However, pollen tubes from its T-DNA insertion mutant (*gdi2b*, SALK_011646), which had T-DNA inserted in the first exon, did not display any obvious phenotype in vitro.

Because no T-DNA insertion mutants were available for RhoGDI2a, we generated RNA interference lines (*gdi2a-RNAi*). Pollens from several independent *gdi2a-RNAi* lines produced 2~3 times thicker pollen tubes than WT tubes (Fig. 7A). This was similar to the pollen-tube phenotype observed when GFP-ROP1 was overexpressed (*12d.8*). *RhoGDI2a* expression was significantly reduced in the mutant pollen grains (Fig. 7B). Consistent with growth depolarization, the localization of endogenous ROPs was depolarized in *gdi2a-RNAi* tubes (Fig. 7C). Interestingly, the growth depolarization of *gdi2a-RNAi* pollen tubes was dependent on the amount of Ca^{2+} in the germination medium, indicating a possible interaction between RhoGDI2a in vivo activity and Ca^{2+} concentration (supplementary material Fig. S4). Introduction of *scn1-1* into the *gdi2a-RNAi* line did not cause a more severe pollen-tube phenotype (Fig. 7A). In addition, double mutant *scn1-1 gdi2b* pollen tubes did not generate obvious growth depolarization (data not shown). These results indicate that RhoGDI2a is the major RhoGDI for the control of apical ROP1 activity in *Arabidopsis* pollen tubes.

Given the high transcript levels of RhoGDI1 and RhoGDI2b, and the expected functional redundancy with RhoGDI2a (supplementary material Fig. S2A), it was surprising that knockdown of only RhoGDI2a significantly promoted the apical ROP1 activation in *Arabidopsis* pollen. A possible explanation for this observation is that RhoGDI1 and RhoGDI2b regulate other types of ROPs in vivo. In *Arabidopsis*, several ROPs distinct from ROP1 are expressed in pollen (Gu et al., 2003). Thus, we do not exclude the possibility that RhoGDI1 and RhoGDI2b might regulate other ROPs in pollen tubes.

Knockdown of RopGAP slightly promotes pollen-tube elongation

We next examined the contribution of RopGAPs to the control of pollen-tube growth by knocking down or knocking out RopGAP1 and RopGAP3. RopGAP1 and RopGAP3 were the only RopGAP members that exhibited detectable expression in our pollen RT-PCR analysis (Fig. 4A). We first observed the in vitro pollen-tube growth of RopGAP1 and RopGAP3 single knockout mutants. *SALK_049590* (*gap1*) and *SALK_056521* (*gap3*) contained T-DNA inserted in the first exons of *RopGAP1* and *RopGAP3*, respectively. In the germination medium containing 0.1 to 10 mM [Ca^{2+}], the growth of *gap1* and *gap3* pollen tubes were not dramatically different from WT tubes: growth depolarization was not observed for either *gap1* or *gap3* tubes. However, *gap3* pollen tubes were slightly longer than WT tubes in low [Ca^{2+}] growth conditions (data not shown). We thus tested the effect of knocking down both *RopGAP1* and *RopGAP3* genes by generating *RopGAP1* and *RopGAP3* double RNA interference lines (*gap1/3-RNAi*). The in vitro cultured *gap1/3-RNAi* pollen tubes appeared longer than WT tubes, but did not display obvious growth depolarization (Fig. 7D). Similarly, we could not observe apparent growth depolarization in the *gap1 gap3* double mutant (data not shown). These observations suggest that knockdown of *RopGAP1* and *RopGAP3* does not affect the apical ROP1 activity significantly enough to induce growth depolarization, but might cause a mild elevation of the apical ROP1 activity to a level that can promote pollen-tube elongation, as seen in low levels of ROP1 overexpression (Gu et al., 2003). These observations are consistent with a biphasic relationship of the apical ROP1 activity with pollen-tube growth behavior (Fig. 1).

The lack of growth depolarization in the *gap1/3-RNAi* lines and *gap1gap3* could be explained by possible weak expression of another RopGAP in pollen that could not be detected by our RT-PCR assay, but could functionally compensate for the loss of RopGAP1 and RopGAP3. However, it is more likely that another class of RhoGAPs has a major role in restricting the apical ROP1 activity. Indeed, we have recently shown that a novel type of RhoGAP, REN1 RhoGAP, is required for the polarity control of pollen-tube growth by globally suppressing ROP1 activity (Hwang et al., 2008). REN1 RhoGAP is localized to the apical region of the pollen-tube PM and to exocytic vesicles accumulated in the tip of pollen tubes. Knockout of REN1 RhoGAP causes drastic depolarization of the apical ROP cap and pollen-tube growth.

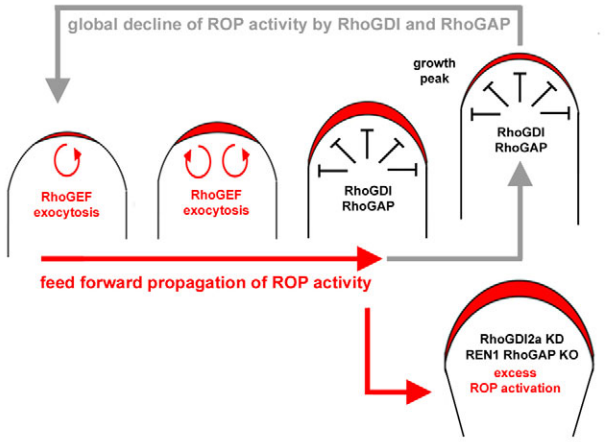

Fig. 8. A model for the generation and maintenance of the apical cap of active ROP1 in growing pollen tubes. The localized ROP1 activity in the center of tube apical PM is amplified through a positive-feedback loop of ROP1 activation, such as recruitment of RhoGEF or other upstream ROP activator, which induces a rapid increase of local ROP1 activity and then its lateral propagation through the apex, generating the active ROP1 cap. The plasma membrane flow driven by active ROP1-mediated exocytosis might also contribute to the rapid lateral propagation of ROP1 activity by facilitating the diffusion of ROP1 and its regulators in the PM. RhoGAP and RhoGDI globally inhibit ROP1 in the apex, preventing excess lateral propagation and finally terminating one cycle of ROP1 activity increase. ROP1 activity starts to increase again, probably via positive feedback from the remnant of the previous active ROP1 cap. A tightly balanced interaction of ROP1 activation and inactivation might continuously generate the dynamic apical ROP1 activity for the continuous tip growth. When the balance is broken by loss of critical RhoGDI or RhoGAP activity (RhoGDI2a and REN1 RhoGAP in *Arabidopsis* pollen tube), ROP1 becomes activated, resulting in the depolarization of apical ROP1 cap and pollen-tube tip growth.

Discussion

Our results in this report provide new insights into the fundamental mechanism enabling a cell to exhibit rapid continuous tip growth. In pollen tubes, we show that the active ROP1 cap determines the growth region and that an optimal size of the active ROP1 cap is generated and maintained for continuous tip growth. Our results

support the hypothesis that the local ROP1 activation is rapidly amplified and spreads laterally to generate the active ROP1 cap, but subsequently ROP1 activity is suppressed by the RhoGAP- and RhoGDI-mediated global inhibition to maintain the proper level and size of active ROP1 cap (Fig. 8). We postulate that the balance between these two counteracting forces supports efficient oscillatory pollen-tube elongation.

This Rho regulatory mechanism might provide a paradigm for the control of tip growth in various systems and cell migration in animals. The ROP1-activity-dependent shift in growth polarity is remarkably similar to cell migration regulated by Rac1 GTPase activity levels (Pankov et al., 2005). Rac1 activity at the leading edge drives cell migration, but excess Rac1 activity induces migrating cells to switch from rapid directional to random movement. Similarly, expression of constitutively active Cdc42 or knockout of RhoGAPs induced the depolarization of growth domain in neurons and fungi (Alberts et al., 2006; Pankov et al., 2005; Ushinsky et al., 2002; Wendland and Philippsen, 2000). Thus, the generation and maintenance of an active Rho-GTPase-containing PM domain that determines the domain for cell expansion or protrusion seems to be a universal mechanism for directional cell expansion and movement. Accordingly, a balance between the propagation of Rho GTPase activation and the global inhibition of Rho GTPase could provide a general mechanism underlying the most efficient cell growth or migration.

Rapid generation of the apical ROP1 cap might involve feed-forward-based lateral amplification of ROP1 activation

Our results suggest that the formation of the apical ROP1 cap involves the lateral propagation of localized ROP1 activity. What is the mechanism underlying this ROP1 propagation? We consider two possible mechanisms that are not mutually exclusive, but might be synergistic. First, the lateral diffusion of active ROP1 and its upstream activators in the tube apical PM could help the ROP1 activity propagate to the whole apex. In growing pollen tubes, as new membrane materials are being added to the tip, the old PM containing active ROP1 is displaced, which might also contribute to lateral movement of active ROP1. This spatial pattern of exocytosis has been recently confirmed by the localization of exocyst to the tip of pollen tubes (Hala et al., 2008) and by FRAP analysis of PM-localized GFP-tagged RLK (Lee et al., 2008). RLK-GFP is targeted to the PM through exocytosis. FRAP analysis of RLK-GFP at the apical PM reveals that RLK-GFP is first targeted to the center of the apical PM and rapidly spreads to the shoulder of the apical RLK-GFP cap, which both temporally and spatially corresponds to the formation of the RIC4 cap. These results support the notion that the center-to-shoulder flow of membrane during pollen-tube growth contributes to the lateral spreading of the apical activated ROP1.

The potential involvement of the tip-targeted exocytosis in the center-to-shoulder spreading of ROP1 activation does not necessarily exclude the existence of other types of exocytosis, e.g. a certain type of rapid exocytosis such as ‘kiss-and-run’ might be directed to the shoulder region. Based on the finding that internalized fluorescent dyes moved to the shoulder of the apex and away from the center of the apex in pollen tubes, Bove and co-workers (Bove et al., 2008), and Zonia and Munnik (Zonia and Munnik, 2008) proposed that exocytosis and endocytosis occur in separate zones: the shoulder and the center of pollen-tube apex, respectively, resulting in PM flow from the shoulder to the center in the pollen-tube apical PM. If such membrane flow occurs in pollen tubes, it would not contribute to the ROP activation propagation that we describe here.

In addition to lateral diffusion or membrane flow, a feed-forward-based amplification of the local ROP1 activation could also contribute to the lateral spreading of the active ROP1. Several lines of evidence support the existence of a feed-forward-based ROP1 activation at the tip of pollen tubes. First, our results in this study show that CA-rop1 expression can induce the activation of endogenous ROP1, supporting a positive-feedback activation of ROP1. Second, we showed that RopGEF1-induced growth depolarization in pollen tubes requires the involvement of active ROP1 (Gu et al., 2006). Last, we showed that active ROP1 promotes the tip-localized F-actin assembly, which in turn is required for the accumulation of active ROP1 in the tube apex, suggesting that ROP1-dependent F-actin is involved in the feed-forward mechanism (Fu et al., 2001; Gu et al., 2005; Hwang et al., 2005). ROP1-dependent F-actin then participates in polarized exocytosis to the apical PM (Lee et al., 2008), which might bring ROP1 activators there to complete the feed-forward ROP1 activation. Therefore, we postulate that the combination of feed-forward-based ROP1 activation with lateral diffusion or displacement of active ROP1 allows rapid generation of the apical ROP1 cap.

Global-inhibition-based balance of ROP1 activity propagation allows rapid tip growth

An increasing number of recent studies reveal the importance of negative regulation of Rho GTPases by both RhoGAPs and RhoGDIs in the control of Rho-GTPase-dependent cell polarity through their roles in spatially restricting Rho GTPases (Carol et al., 2005; Jenkins et al., 2006; Ohta et al., 2006; Saito et al., 2007). In non-plant systems, these negative regulators often act as lateral inhibitors by localizing to the region of the cell where the Rho GTPase activity is excluded (Jenkins et al., 2006; Ohta et al., 2006; Saito et al., 2007). By contrast, our findings suggest that both RhoGAPs and RhoGDIs act globally in maintaining the active ROP1 cap to a proper level and size during rapid continuous tip growth. Overexpression of RopGAP1 or RhoGDI1 suppressed the enlargement of active ROP1 cap induced by ROP1 overexpression (Fig. 5). Loss of RhoGDI2a caused enlargement of the apical ROP1 cap and depolarized growth in *Arabidopsis* pollen tubes (Fig. 7A,C). Similarly, knockout of a pollen-specific novel GAP for ROP1, REN1, also causes the enlargement of the apical ROP1 cap and growth depolarization in *Arabidopsis* pollen tubes (Hwang et al., 2008). The global effects of these negative regulators are supported by the localization of RhoGDIs and RopGAPs either evenly in the cytosol or to the apical PM as the active ROP1 does. Their localization patterns are consistent with their function in similarly downregulating both the amplitude and the size of the active ROP1 apical cap.

Recently, it has been proposed that tobacco RhoGAP1 acts as a lateral inhibitor to limit ROP GTPase activation to the tobacco pollen-tube tip (Klahre and Kost, 2006). When transiently expressed, tobacco RhoGAP1-YFP was preferentially localized to the tube subapical PM and induced the formation of thinner pollen tubes (Klahre and Kost, 2006). In addition, the involvement of subapically localized PI-PLCs in the maintenance of tip-localized growth area has been proposed in tobacco and petunia (Dowd et al., 2006; Helling et al., 2006). The contribution of these proteins to the maintenance of the tip-localized ROP activity needs to be further evaluated via a loss-of-function approach. Nonetheless, lateral inhibitions might aid the global inhibition by RhoGDI and RhoGAP

for more efficient restriction of ROP1 activity to the pollen-tube apex.

Several functions of RhoGDI have been proposed: removal of RhoGTPase from the PM, and targeting Rho to the active site, and promoting local turnover rate of Rho. Our study of RhoGDI supports the idea that the primary function of RhoGDIs in the control of the apical ROP activity in pollen-tube growth is the removal of Rho GTPases from the PM by sequestering the majority of Rho in the cytosol (Figs 4-7). The overexpression of RhoGDI1 restored both the apical ROP activity and pollen-tube growth of ROP1-overexpressing pollen tubes to those of control tubes (Fig. 5). The reduction of ROP activity in the apical PM was primarily global: both the amplitude and width of bell-shaped distribution of active ROP were globally reduced in normally growing pollen tubes and also in pollen tubes expressing RhoGDI1 (Figs 2,4,5). Therefore, once inactivated by RhoGAP, ROP1 GTPase is probably removed from the pollen-tube apical PM indiscriminately by RhoGDIs and sequestered in the cytosol until it is recruited to the apical growth area. However, further study is required to examine whether RhoGDIs also have a role in targeting ROP to specific sites, or in promoting ROP GTPase turnover rate in pollen tubes.

Global downregulation of ROP1 signaling might be linked to the negative feedback for the self-organization of pollen-tube growth

The need for global downregulation of ROP1 might be linked to the self-organizing mechanism underlying uniform radial expansion and growth oscillation in pollen tubes. During pollen-tube growth, the diameter of the tube (or the ROP1 maximum cap site) is maintained, and elongation is often oscillatory, suggesting a self-organizing mechanism for the regulation of pollen-tube growth, i.e. a requirement for positive- and negative-feedback regulations (Hwang et al., 2005). RhoGAP- and RhoGDI-mediated global inhibition of ROP1 activity might provide a convenient mechanism linking negative-feedback regulations to these global inhibitors. Indeed, evidence suggests that the REN1 RhoGAP is subject to negative-feedback regulation (Hwang et al., 2008). A key ROP1 downstream signaling event that might participate in the negative feedback is the ROP1-dependent Ca^{2+} accumulation in the tip of pollen tubes (Gu et al., 2005; Li et al., 1999). In support of Ca^{2+}-mediated negative feedback, we found that growth depolarization of *gdi2a-RNAi* pollen tubes was more severe when [Ca^{2+}] was low in the germination medium, whereas high [Ca^{2+}] in the medium completely suppressed the *gdi2a-RNAi* induced growth depolarization (supplementary material Fig. S4). It will be intriguing to see whether ROP1 activation regulates RhoGDI2a via a Ca^{2+}-mediated mechanism. Future studies of the molecular mechanisms by which ROP1 regulators are controlled will help us to understand how the proper level of ROP1 activity is sustained in the tube apex for rapid tip growth.

Materials and Methods

Plant materials

Arabidopsis (*Arabidopsis thaliana*, Columbia ecotype) and tobacco (*Nicotiana tabacum*) plants were grown in a growth room or a growth chamber with a 16 hour photoperiod at 22°C.

Transient expression in tobacco pollen

Arabidopsis ROP1 and its regulators were transiently expressed in tobacco pollen as described (Fu et al., 2001). Usually, 0.5 μg of pollen expression constructs were used to coat gold particles (d=1 μm) if not indicated. GFP or GFP-RIC4ΔC constructs (0.1~0.2 μg) were co-transformed as an internal control or an active ROP1 reporter, respectively. The pollen-tube growth and in vivo ROP1 activity were measured 3-7 hours after bombardment, when the majority of pollen tubes display rapid tip growth, and ballooning of the pollen-tube tip by ROP overexpression was still in progress.

Confocal laser scanning microscopy

The transformed pollen tubes were observed with a Bio-Rad MRC 600 (Bio-Rad Laboratories, Hercules, CA) or a Leica SP2 (Leica, Wetzlar, Germany) confocal microscope. In each set of experiments, pollen tubes with moderate levels of GFP or YFP fluorescence were chosen and confocal images were taken from the longitudinal medial plane through the pollen-tube tip, applying the same CLSM setting.

Analysis of pollen-tube growth and ROP activity

The pollen-tube growth and ROP1 activity were analyzed by using a Metamorph software (Version 4.5, Universal Imaging, West Chester, PA) and ImageJ (http://rsb.info.nih.gov/ij) as described in the previous report (Hwang et al., 2005).

We assume that a pollen tube is a cylinder with a hemisphere at the tip and active ROPs are distributed in the hemispherical PM, forming a symmetric gradient from the very summit. Thus, the pollen-tube growth (Δsurface area) is linearly proportional to the linear elongation rate of pollen tubes (Δtube length). Likewise, the broadness of active ROP1 cap (surface area of apical PM with active ROP1) and the mean amount of active ROP1 in the pollen-tube tip are linearly proportional to the distance of the apical PM region with active ROP localization and the mean amount of active ROP1 in the region in a single median section of the pollen-tube apical PM. Therefore, the relationship between ROP activity and pollen-tube growth measured in 2D images of pollen tubes reflects the relationship between them well in the 3D pollen-tube system.

From the median CLSM scans, the distance from the pollen grain to the pollen-tube tip was measured as the pollen-tube length and the widest diameter of the pollen-tube tip was measured as the pollen-tube width. The pollen-tube growth rate was measured as a net tube elongation from sequential CLSM images of a growing pollen tube.

Because GFP-RIC4ΔC localization to the apical PM illustrates in vivo ROP1 activity in the pollen-tube apex, three features of the apical ROP1 activity were measured by quantifying GFP-RIC4ΔC localization from median sectioned CLSM images of pollen tubes: the size of active ROP1 apical cap, the mean ROP1 activity and the total ROP1 activity in the cap. (1) The size of active ROP1 cap, which indicates the broadness of active ROP1 localization in the tube apical PM, was quantified by measuring the distance of the PM region with distinct GFP-RIC4ΔC signal. (2) The mean ROP1 activity in the apical cap was quantified by measuring the mean intensity of GFP-RIC4ΔC in the PM region (I-pm). I-pm was calculated as a line average of GFP intensity drawn along the PM area with distinct GFP-RIC4ΔC localization, which was standardized with the average GFP intensity in the cytosol (I-pm as a percentage of I-cyt). I-cyt was measured as a mean GFP intensity from a circle of d=5 μm drawn in the center of tube apex (Fig. 1B). In tubes with no distinct PM localization of GFP-RIC4ΔC (the cap size=0), I-pm was measured from the center of tube apical PM (~6 μm), which was 70-90% of I-cyt. (3) The total ROP1 activity in the active ROP1 cap was estimated by multiplying I-pm/I-cyt by the cap size. The significance of differences in pollen-tube growth and in apical ROP activity between different samples was tested usually by using *t*-test. The coefficient and significance of correlation between pollen-tube width and size of apical ROP1 cap were calculated by using Pearson correlation.

Analysis of intensity profiles of GFP-RIC4ΔC localized in the apical PM

In most of cases in which we compared the broadness and mean or total levels of ROP activity in accordance to the broadness of growth area (tube width) or pollen-tube elongation rate, we measured the three aspects of ROP1 activity using GFP-RIC4ΔC, as described above. However, when we analyzed the spatiotemporal changes in apical ROP1 activity in individual pollen tubes, we obtained the intensity profiles of GFP-RIC4ΔC along the apical PM by using linescan function of ImageJ. The resultant profiles were then fitted by using Gaussian curve fit function of Origin software (Micrococal Origin 7, Originlab Corporation, Northampton, MA). The calculated amplitudes and widths from the Gaussian fit are considered to represent the peak level and the broadness of apical ROP1 activity, respectively.

Generation of RopGAP and RhoGDI RNA interference and screen of T-DNA knockout lines

To generate RopGAP1 and RopGAP3 double RNAi construct (*gap1/3-RNAi*), a chimeric cDNA of RopGAP1 (1-298 nt of the coding sequence) and RopGAP3 (1-304 nt) were cloned in a pFGC5941dsRNA vector behind the *LAT52* promoter [the *Arabidopsis* Biological Resource Center (ABRC) accession no. CD3-447]. For the *RhoGDI2a* RNAi construct (*gdi2a-RNAi*), 68-560 nt of the *RhoGDI2a* coding sequence was cloned in a pGSA1285 dsRNA vector behind the *LAT52* promoter (ABRC accession no. CD3-454). *Arabidopsis* plants were transformed using *Agrobacterium*-mediated method (Clough and Bent, 1998). In vitro pollen-tube phenotype was analyzed in homozygote T2 or T3 plants. More than five independent transformed lines were analyzed and found to have the same pollen-tube growth phenotype. SALK T-DNA insertion mutants were ordered from ABRC (Alonso et al., 2003), and the T-DNA insertion site was analyzed using the gene-specific and T-DNA left border primers.

Reverse transcriptase (RT)-PCR analysis

Total RNA was isolated from *Arabidopsis* pollen or flowers using TRIZOL reagent (Invitrogen). From 0.1-0.3 μg of total RNA, cDNA was generated with Invitrogen

SuperScript™II RNase H- RT system. One tenth of the RT reaction was used for PCR with gene specific primers. The gene specific primers are as followed. RopGAP1 (ccgatggaggagaagaagac and cttgataagccctgccaaac), RopGAP2 (atttcgtccgccgttcatc and ttcttcttcaacaacatcagcc), RopGAP3 (aatccagacaacggcaaag and gcccaatcaagaatcgcag), RopGAP4 (gagagtgaagatgagtgtgtgg and ggatttgaggctggaaccaac), RopGAP5 (ccaaccaatatccgccacg and aatcctcatctgactcacactg), RopGAP6 (cattagtcgcccaaccaatatc and caaccttcacaaaatcctccc), RhoGDI1 (atgtctttggtatctggagcc and aagcgcaggccattctttac), RhoGDI2a (atggttttggaagatgagatg and ttgccaactcttgcggatgtc) and RhoGDI2b (atggttttgaacgatgaggag and cagccaatttttgccaatgtc). The expression of *ACTIN3* was detected as an internal control.

Pollen grains were isolated from open *Arabidopsis* flowers (stage 14). Pollen was purified by vortexing collected flowers in liquid germination medium with DEPC and filtering released pollen grains through a Nitex mesh (pore size=250 μm). After gentle rinsing with fresh DEPC-germination medium, pollen grains were suspended in TRIZOL reagent. The purity of pollen grains isolated with this protocol was higher than 99%.

Observation of in vitro cultured *Arabidopsis* pollen tubes

Open flowers (stage 14) were collected and allowed to dry for 1.5 hours at room temperature (RT). Mature pollen grains were dusted and germinated on a standard germination medium containing 2 mM $[Ca^{2+}]_{ext}$ as described (Li et al., 1999). Pollen tubes were observed over 2-19 hours with an inverted microscope (Nikon eclipse TE300, Tokyo, Japan) and pictures taken using a cooled CCD camera (Hamamatsu CA4742-95, Hamamatsu City, Japan) attached to the microscope. The tube length and width were measured with a Metamorph software.

Immunolocalization of endogenous ROPs

Immunostaining of *Arabidopsis* pollen tubes with anti-ROP antibodies was performed as described (Lin et al., 1996). *Arabidopsis* pollen tubes cultured for 3 hours on a thin layer of germination agar medium were fixed with 4% paraformaldehyde solution for 2 hours at RT. After cell wall was digested with 2% cellulase solution, pollen tubes were incubated with anti-ROP antibody in PBS and 1% nonfat milk at 4°C overnight and then with a secondary antibody (FITC-conjugated goat anti-rabbit IgG, Sigma) at RT for 2 hours.

This work is supported by grants from the National Institutes of Health, Department of Energy and National Science Foundation to Z.Y. We thank members of the Yang laboratory for technical assistance and stimulating discussion during the course of this work. Deposited in PMC for release after 12 months.

Supplementary material available online at
http://jcs.biologists.org/cgi/content/full/123/3/340/DC1

References

Alberts, P., Rudge, R., Irinopoulou, T., Danglot, L., Gauthier-Rouviere, C. and Galli, T. (2006). Cdc42 and actin control polarized expression of TI-VAMP vesicles to neuronal growth cones and their fusion with the plasma membrane. *Mol. Biol. Cell* **17**, 1194-1203.

Alonso, J. M., Stepanova, A. N., Leisse, T. J., Kim, C. J., Chen, H., Shinn, P., Stevenson, D. K., Zimmerman, J., Barajas, P., Cheuk, R. et al. (2003). Genome-wide insertional mutagenesis of Arabidopsis thaliana. *Science* **301**, 653-657.

Bischoff, F., Vahlkamp, L., Molendijk, A. and Palme, K. (2000). Localization of AtROP4 and AtROP6 and interaction with the guanine nucleotide dissociation inhibitor AtRhoGDI1 from Arabidopsis. *Plant Mol. Biol.* **42**, 515-530.

Bove, J., Vaillancourt, B., Kroeger, J., Hepler, P. K., Wiseman, P. W. and Geitmann, A. (2008). Magnitude and direction of vesicle dynamics in growing pollen tubes using spatiotemporal image correlation spectroscopy and fluorescence recovery after photobleaching. *Plant Physiol.* **147**, 1646-1658.

Bushart, T. J. and Roux, S. J. (2006). Conserved features of germination and polarized cell growth: a few insights from a pollen-fern spore comparison. *Ann Bot. (Lond.)* **99**, 9-17.

Butty, A. C., Perrinjaquet, N., Petit, A., Jaquenoud, M., Segall, J. E., Hofmann, K., Zwahlen, C. and Peter, M. (2002). A positive feedback loop stabilizes the guanine-nucleotide exchange factor Cdc24 at sites of polarization. *EMBO J.* **21**, 1565-1576.

Carol, R. J., Takeda, S., Linstead, P., Durrant, M. C., Kakesova, H., Derbyshire, P., Drea, S., Zarsky, V. and Dolan, L. (2005). A RhoGDP dissociation inhibitor spatially regulates growth in root hair cells. *Nature* **438**, 1013-1016.

Clough, S. J. and Bent, A. F. (1998). Floral dip: a simplified method for Agrobacterium-mediated transformation of Arabidopsis thaliana. *Plant J.* **16**, 735-743.

Dowd, P. E., Coursol, S., Skirpan, A. L., Kao, T. H. and Gilroy, S. (2006). Petunia phospholipase c1 is involved in pollen tube growth. *Plant Cell* **18**, 1438-1453.

Franklin-Tong, V. E. (1999). Signaling and the modulation of pollen tube growth. *Plant Cell* **11**, 727-738.

Fu, Y., Wu, G. and Yang, Z. (2001). Rop GTPase-dependent dynamics of tip-localized F-actin controls tip growth in pollen tubes. *J. Cell Biol.* **152**, 1019-1032.

Govek, E. E., Newey, S. E. and Van Aelst, L. (2005). The role of the Rho GTPases in neuronal development. *Genes Dev.* **19**, 1-49.

Gu, Y., Vernoud, V., Fu, Y. and Yang, Z. (2003). ROP GTPase regulation of pollen tube growth through the dynamics of tip-localized F-actin. *J. Exp. Bot.* **54**, 93-101.

Gu, Y., Fu, Y., Dowd, P., Li, S., Vernoud, V., Gilroy, S. and Yang, Z. (2005). A Rho family GTPase controls actin dynamics and tip growth via two counteracting downstream pathways in pollen tubes. *J. Cell Biol.* **169**, 127-138.

Gu, Y., Li, S., Lord, E. M. and Yang, Z. (2006). Members of a novel class of Arabidopsis Rho guanine nucleotide exchange factors control Rho GTPase-dependent polar growth. *Plant Cell.* **18**, 366-381.

Hála, M., Cole, R., Synek, L., Drdová, E., Peenková, T., Nordheim, A., Lamkemeyer, T., Madlung, J., Hochholdinger, F., Fowler, J. E. and Zársky, V. (2008). An exocyst complex functions in plant cell growth in *Arabidopsis* and tobacco. *Plant Cell.* **20**, 1330-1345.

Helling, D., Possart, A., Cottier, S., Klahre, U. and Kost, B. (2006). Pollen tube tip growth depends on plasma membrane polarization mediated by tobacco PLC3 activity and endocytic membrane recycling. *Plant Cell* **18**, 3519-3534.

Hepler, P. K., Vidali, L. and Cheung, A. Y. (2001). Polarized cell growth in higher plants. *Annu. Rev. Cell Dev. Biol.* **17**, 159-187.

Hwang, J. U., Gu, Y., Lee, Y. J. and Yang, Z. (2005). Oscillatory ROP GTPase activation leads the oscillatory polarized growth of pollen tubes. *Mol. Biol. Cell* **16**, 5385-5399.

Hwang, J. U., Vernoud, V., Szumlanski, A., Nielsen, E. and Yang, Z. (2008). A tip-localized RhoGAP controls cell polarity by globally inhibiting Rho GTPase at the cell apex. *Curr. Biol.* **18**, 1907-1916.

Jenkins, N., Saam, J. R. and Mango, S. E. (2006). CYK-4/GAP provides a localized cue to initiate anteroposterior polarity upon fertilization. *Science* **313**, 1298-1301.

Klahre, U. and Kost, B. (2006). Tobacco RhoGTPase activating Protein1 spatially restricts signaling of RAC/Rop to the apex of pollen tubes. *Plant Cell* **18**, 3033-3046.

Kost, B., Lemichez, E., Spielhofer, P., Hong, Y., Tolias, K., Carpenter, C. and Chua, N. H. (1999). Rac homologues and compartmentalized phosphatidylinositol **4**, 5-bisphosphate act in a common pathway to regulate polar pollen tube growth. *J. Cell Biol.* **145**, 317-330.

Lee, Y. J., Szumlanski, A., Nielsen, E. and Yang, Z. (2008). Rho-GTPase-dependent F-actin dynamics coordinate vesicle targeting and exocytosis during tip growth. *J. Cell Biol.* **181**, 1155-1168.

Li, H., Lin, Y., Heath, R. M., Zhu, M. X. and Yang, Z. (1999). Control of pollen tube tip growth by a Rop GTPase-dependent pathway that leads to tip-localized calcium influx. *Plant Cell* **11**, 1731-1742.

Li, R., Zhang, B. and Zheng, Y. (1997). Structural determinants required for the interaction between Rho GTPase and the GTPase-activating domain of p190. *J. Biol. Chem.* **272**, 32830-32835.

Lin, Y. and Yang, Z. (1997). Inhibition of pollen tube elongation by microinjected Anti-Rop1Ps antibodies suggests a crucial role for Rho-type GTPases in the control of tip growth. *Plant Cell* **9**, 1647-1659.

Lin, Y., Wang, Y., Zhu, J. K. and Yang, Z. (1996). Localization of a Rho GTPase implies a role in tip growth and movement of the generative cell in pollen tubes. *Plant Cell* **8**, 293-303.

Lord, E. M. and Russell, S. D. (2002). The mechanisms of pollination and fertilization in plants. *Annu. Rev. Cell Dev. Biol.* **18**, 81-105.

Ohta, Y., Hartwig, J. H. and Stossel, T. P. (2006). FilGAP, a Rho- and ROCK-regulated GAP for Rac binds filamin A to control actin remodelling. *Nat. Cell Biol.* **8**, 803-814.

Ozbudak, E. M., Becskei, A. and van Oudenaarden, A. (2005). A system of counteracting feedback loops regulates Cdc42p activity during spontaneous cell polarization. *Dev. Cell* **9**, 565-571.

Pankov, R., Endo, Y., Even-Ram, S., Araki, M., Clark, K., Cukierman, E., Matsumoto, K. and Yamada, K. M. (2005). A Rac switch regulates random versus directionally persistent cell migration. *J. Cell Biol.* **170**, 793-802.

Parker, J. S., Cavell, A. C., Dolan, L., Roberts, K. and Grierson, C. S. (2000). Genetic interactions during root hair morphogenesis in Arabidopsis. *Plant Cell* **12**, 1961-1974.

Saito, K., Fujimura-Kamada, K., Hanamatsu, H., Kato, U., Umeda, M., Kozminski, K. G. and Tanaka, K. (2007). Transbilayer phospholipid flipping regulates Cdc42p signaling during polarized cell growth via Rga GTPase-activating proteins. *Dev. Cell* **13**, 743-751.

Ushinsky, S. C., Harcus, D., Ash, J., Dignard, D., Marcil, A., Morchhauser, J., Thomas, D. Y., Whiteway, M. and Leberer, E. (2002). CDC42 is required for polarized growth in human pathogen Candida albicans. *Eukaryot. Cell* **1**, 95-104.

Wedlich-Soldner, R., Altschuler, S., Wu, L. and Li, R. (2003). Spontaneous cell polarization through actomyosin-based delivery of the Cdc42 GTPase. *Science* **299**, 1231-1235.

Weiner, O. D., Neilsen, P. O., Prestwich, G. D., Kirschner, M. W., Cantley, L. C. and Bourne, H. R. (2002). A PtdInsP(3)- and Rho GTPase-mediated positive feedback loop regulates neutrophil polarity. *Nat. Cell Biol.* **4**, 509-513.

Wendland, J. and Philippsen, P. (2000). Determination of cell polarity in germinated spores and hyphal tips of the filamentous ascomycete Ashbya gossypii requires a rhoGAP homolog. *J. Cell Sci.* **113**, 1611-1621.

Wu, G., Li, H. and Yang, Z. (2000). Arabidopsis RopGAPs are a novel family of rho GTPase-activating proteins that require the Cdc42/Rac-interactive binding motif for rop-specific GTPase stimulation. *Plant Physiol.* **124**, 1625-1636.

Wu, G., Gu, Y., Li, S. and Yang, Z. (2001). A genome-wide analysis of Arabidopsis Rop-interactive CRIB motif-containing proteins that act as Rop GTPase targets. *Plant Cell* **13**, 2841-2856.

Xu, J., Wang, F., Van Keymeulen, A., Herzmark, P., Straight, A., Kelly, K., Takuwa, Y., Sugimoto, N., Mitchison, T. and Bourne, H. R. (2003). Divergent signals and cytoskeletal assemblies regulate self-organizing polarity in neutrophils. *Cell* **114**, 201-214.

Zonia, L. and Munnik, T. (2008). Vesicle trafficking dynamics and visualization of zones of exocytosis and endocytosis in tobacco pollen tubes. *J. Exp. Bot.* **59**, 861-873.